



Nanocomposite of attapulgite–Ag₃PO₄ for Orange II photodegradation

Jianfeng Ma ^{a,b,*}, Jing Zou ^a, Liangyin Li ^a, Chao Yao ^a, Yong Kong ^a, Bingying Cui ^a, Runliang Zhu ^c, Dinglong Li ^a

^a School of Environmental and Safety Engineering, Changzhou University, Jiangsu 213164, China

^b State Key Laboratory of Silicon Materials, Zhejiang University, Hangzhou 310027, China

^c Guangzhou Institute of Geochemistry, Chinese Academy of Sciences, Guangzhou 510640, China

ARTICLE INFO

Article history:

Received 18 March 2013

Received in revised form 17 June 2013

Accepted 21 June 2013

Available online 29 June 2013

Keywords:

Silver phosphate

Nanocomposites

Attapulgite

Wastewater treatment

ABSTRACT

Well-spread Ag₃PO₄ particles (5 nm in size) were synthesized on the surface of attapulgite (ATP) for the sunlight-driven catalytic removal of Orange II from water. The attapulgite–Ag₃PO₄ composites were characterized by XRD, XRF, XPS and UV-vis diffuse reflectance spectroscopy. The Ag₃PO₄ nanoparticles were successfully loaded onto the ATP surface with a uniform distribution of spherical particles without any evident aggregation. The photocatalytic activity and stability of Ag₃PO₄ were significantly improved by loading on ATP. In addition, the silver content in the photocatalyst composite decreased from 77.3 wt% in bare Ag₃PO₄ to 18.8 wt% in the composite, which will greatly decrease the cost of the treatment. Although Ag₃PO₄ precipitated quickly in aqueous solution, the results showed that it also can be applied as a coating onto the carriers, which can avoid the aggregation of nanoparticles into micrometer-sized particles in solutions.

© 2013 Elsevier B.V. All rights reserved.

1. Introduction

Ag₃PO₄ exhibits extremely high photocatalytic efficiency for organic dye decomposition under visible light irradiation [1–6]. The particle size of Ag₃PO₄ evidently affects dye degradation [1]. Dinh et al. [1] synthesized silver orthophosphate nanocrystals in the range of 8 nm to 16 nm that demonstrated superior photocatalytic activity under visible light compared with micron-sized Ag₃PO₄ particles. Oleylamine was used as solvent to synthesize the nano-sized Ag₃PO₄ particles in 5–10 nm [7]. However, the nanoparticles aggregated quickly into micrometer-sized particles in aqueous solutions, thereby hindering their practical applications. Recently, more and more studies have focused on the suitable supporter for catalyst to enhance application of photocatalysts [8].

In the past two years, considerable efforts have been exerted in developing a suitable supporter for Ag₃PO₄ particles. Some supports such as flaky-layered double hydroxides [4], TiO₂ [6], AgCl [9], carbon quantum dots [10], graphene oxide [11], and SnO₂ [12] were studied to improve the dispersion of Ag₃PO₄ particles. The particles sizes were controlled within 200–300 nm [4,6,9–11] and even within 700–800 nm [12]. However, further reduction of the

particle size into several nanometers has a great potential. Cheap and abundant supports such as clay should also be developed for Ag₃PO₄ catalysts.

Clays have been used as natural, cost-effective adsorbent and supporter for catalysis in wastewater treatment. Bentonite, with layered structure, has been successfully investigated as Ag₃PO₄ carrier for dye wastewater treatment [13]. Attapulgite (ATP; also called palygorskite), with special lath-like or fibrous morphology, is a species of hydrated magnesium aluminum silicate non-metallic mineral [14]. Given its unique structure and considerable textual properties, natural ATP is widely used as adsorbents, adhesives, catalysts, and catalyst supports [14,15]. It has large surface area exhibiting excellent activity and chemical adsorption property. Liu et al. [16] prepared ATP/Fe₃O₄ composites by a co-precipitation technique and found that the composite showed enhanced magnetic properties. Zhang et al. [17] obtained ATP/SnO₂–TiO₂ via an in situ sol–gel method and investigated its photocatalytic removal ability of the methyl orange under ultraviolet radiation. In this study, ATP was used as Ag₃PO₄ supporter because of its high specific surface area and nano-fibrous morphology.

Ag₃PO₄ is easily precipitated in the solution, and the crystal particle sizes are estimated to be approximately 0.5–2 μm [2]. The large-sized particles that are quickly precipitated have difficulty anchoring onto the supporter. Khan et al. reported a colloidal approach to synthesize highly uniform and spherical silver phosphate with the size of ~200 nm [18]. With the colloidal synthesis approach, the colloidal Ag₃PO₄ may be coat on the supporter in thin film.

* Corresponding author at: School of Environmental and Safety Engineering, Changzhou University, Jiangsu 213164, China. Tel.: +86 519 86330086; fax: +86 519 86330083.

E-mail address: jma@zju.edu.cn (J. Ma).

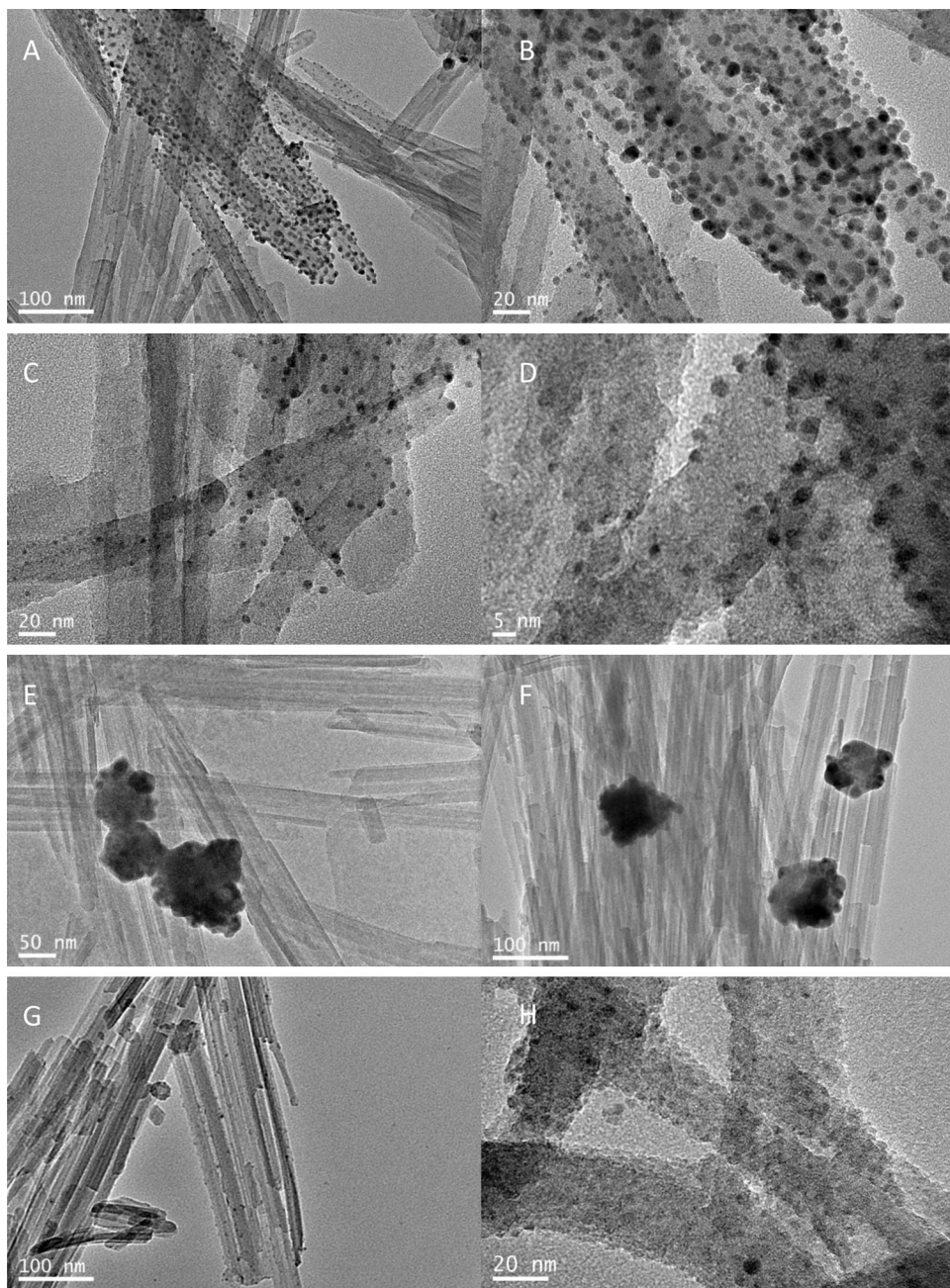


Fig. 1. TEM images of Ag₃PO₄-ATP-Co (A–D), Ag₃PO₄-ATP-Pr (E and F) and recycled Ag₃PO₄-ATP-Co (G and H).

In this study, Ag₃PO₄-ATP composites were synthesized. Colloidal Ag₃PO₄ was used as a precursor to obtain the coated crystalline grains of Ag₃PO₄ on ATP. With the method, Ag₃PO₄ can be applied as a coating onto many kinds of carriers, e.g., clay, silica, and active carbon.

2. Experimental

2.1. Synthesis

ATP, more than 90% of purity levels with an average particle size of 200 mesh, was provided by Jiangsu ATP Co. Ltd. in Xuyi, China. The BET surface area of original ATP is 124 m²/g, and the BJH adsorption cumulative volume of pores is 0.48 cm³/g.

Colloidal Ag₃PO₄ was synthesized according to the method described by Khan et al. [18]. The concentrations of disodium hydrogen phosphate hydrate (A.R.) and silver nitrate (A.R.) were both adjusted to 0.02 mol/L. Each reactant solution was mixed thoroughly, and the resulting solution was stirred for 1 h (no precipitation was found, but colloid was observed). ATP was added to the colloid and stirring was performed for 3 h. Afterwards, the mixture was centrifuged, collected, and dried at 70 °C for 12 h.

The precipitation method was also used to synthesize Ag₃PO₄-ATP for comparison. The difference between the colloidal and precipitation methods was the concentrations of disodium hydrogen phosphate hydrate and silver nitrate, i.e., 0.02 mol/L for the colloidal method and 0.1 mol/L for the precipitation method. The sample collected from the colloid method was identified

by Ag_3PO_4 –ATP–Co, whereas the other sample was identified by Ag_3PO_4 –ATP–Pr using the precipitation method.

2.2. Characterization

The high-resolution transmission electron microscopy (HRTEM) was performed by JEOL JEM-2100 LaB6 Transmission Electron Microscope (Japan). X-ray diffraction (XRD) patterns of the prepared samples were determined using an X-ray diffractometer (Max-2550PC, Rigaku D) with $\text{Cu K}\alpha$ radiation (40 kV, 300 mA) at 0.154 nm to confirm the structure of the materials. All XRD patterns were obtained from 0.5° to 80° with a scan speed of $4^\circ/\text{min}$. Ultraviolet–visible (UV-vis) diffusion reflectance spectra were recorded using a UV-vis spectrometer (UV-2450, Shimadzu) and converted to absorption spectra by the standard Kubelka–Munk method. Specific surface areas of the prepared photocatalysts were measured using the Brunauer, Emmett, and Teller (BET) method (Autosorb-iQ2-MP, Quantachrome Instruments). X-ray fluorescence (XRF, Horiba XGT-1000WR) was used to determine the silver content in the products.

2.3. Photocatalytic activity testing

A mixture of Orange II solutions (70 mg/L, 500 mL) and the given photocatalyst (Ag_3PO_4 –ATP–Co, Ag_3PO_4 –ATP–Pr, or Ag_3PO_4) was magnetically stirred in the absence of light for 60 min to ensure adsorption–desorption equilibrium. The weight of all solid powders was 200 mg/L. The mixture was then stirred under visible light irradiation using a 300 W Xe arc lamp or natural sunlight at about 900–1000 lux (as tested by a Digital Lux meter TES-1339, Shanghai, China). Considering the time intervals, 5 mL of the suspension was collected and centrifuged to remove the photocatalyst particles.

2.4. Stability testing

To evaluate the stability and recyclability of the composites, the suspension was centrifuged at the end of each cycle and then the supernatant was analyzed and discarded. The dose of Ag_3PO_4 –ATP–Co, Ag_3PO_4 –ATP–Pr, and Ag_3PO_4 were all 200 mg/L.

3. Results and discussion

3.1. Catalyst characterization

3.1.1. HRTEM

Fig. 1 shows the HRTEM images of Ag_3PO_4 –ATP–Co and Ag_3PO_4 –ATP–Pr composites. ATP clearly exhibited a fibrous structure, and some fibers formed straight parallel aggregates and rods. Fig. 1A and B shows that after covering with colloid Ag_3PO_4 , the Ag_3PO_4 nanoparticles were successfully loaded onto the ATP surface. The sample showed a uniform distribution of spherical particles without any evident aggregation. Based on Fig. 1C and D, the particles were estimated to have an average size of about 2.5–5 nm, and observed to be evenly dispersed on the surface of the ATP fibers. On the other hand, Ag_3PO_4 particles synthesized by simple precipitation (Fig. 1E and F) had particle sizes of >100 nm, and were not evenly dispersed on the ATP surface. After it was recycled for four runs, the HRTEM images of the recycled Ag_3PO_4 –ATP–Co show that the fine particles still covered the surface of ATP and no aggregated particle was observed.

3.1.2. Specific surface area

BET is the most common method used to describe specific surface area. The BET surface area of the original ATP is $124 \text{ m}^2/\text{g}$. The BJH adsorption cumulative volume of pores is $0.48 \text{ cm}^3/\text{g}$. The specific surface area of the Ag_3PO_4 particles is $23.5 \text{ m}^2/\text{g}$. When

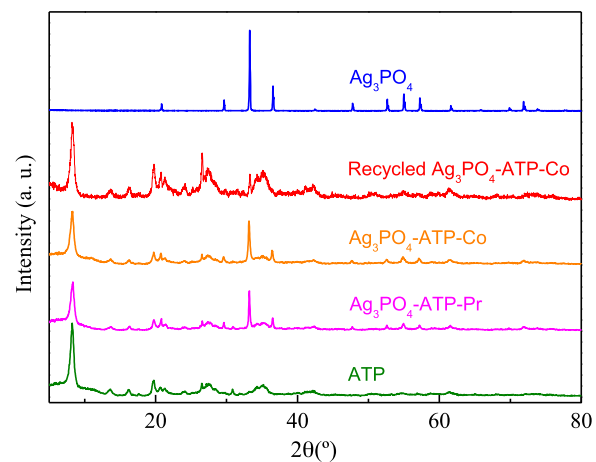


Fig. 2. X-ray diffraction patterns of natural ATP, Ag_3PO_4 , Ag_3PO_4 –ATP–Co, Ag_3PO_4 –ATP–Pr and recycled Ag_3PO_4 –ATP–Co.

Ag_3PO_4 covered the surface of ATP, its specific surface area of Ag_3PO_4 –ATP–Pr increased to $189 \text{ m}^2/\text{g}$, whereas the specific surface area of Ag_3PO_4 –ATP–Co increased to $365 \text{ m}^2/\text{g}$.

3.1.3. XRD spectra

The samples are also analyzed by X-ray powder diffraction (XRD) and the patterns of ATP, Ag_3PO_4 , Ag_3PO_4 –ATP–Co and Ag_3PO_4 –ATP–Pr composites are presented in Fig. 2. The diffraction peaks at $2\theta = 8.3, 13.6, 19.7$, and 26.6° correspond to the primary diffraction of the (110), (200), (040), and (400) planes of ATP, respectively.

For free Ag_3PO_4 particles, all the diffraction peaks are well indexed as diffraction peaks of cubic Ag_3PO_4 (JCPDS No. 06-0505). Fig. 2 shows that all of the diffraction peaks of Ag_3PO_4 –ATP–Co and Ag_3PO_4 –ATP–Pr could be indexed to the body-centered cubic Ag_3PO_4 (JCPDS No. 06-0505). A typical diffraction peak of ATP at 8.3° , which corresponds to a basal spacing of 1.04 nm , is evident according to Fig. 2. After coated with Ag_3PO_4 , this peak appears also at 8.3° correspondingly, which inferred that all the reactions can just occur on the surface of ATP during the composite process without destroying the crystalline structure of it. The similarity of the XRD patterns between Ag_3PO_4 –ATP–Co and Ag_3PO_4 –ATP–Pr indicates that there are Ag_3PO_4 existed on the surface of ATP by both coating method. After it was recycled for four runs, the XRD pattern of recycled Ag_3PO_4 –ATP–Co showed that the typical peak still appeared at 33.3° (JCPDS No. 06-0505).

3.1.4. XRF

The chemical compositions of attapulgite before and after covered with Ag_3PO_4 were determined by XRF analysis (Table 1). The results showed that silicate was the prevalent component of natural ATP. Iron was the second most abundant component, whereas metals such as K, Ca and Na and other metal elements were present in trace amounts.

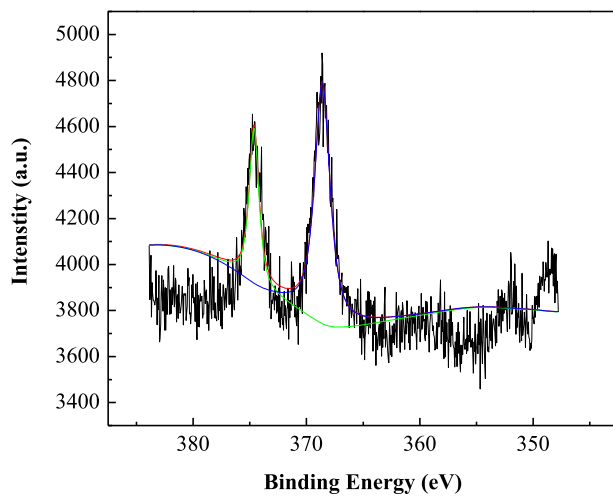
After covered with Ag_3PO_4 (Ag_3PO_4 –ATP–Co), a silver content of 18.87 wt% was found. However, the composites synthesized by precipitation method only comprised 8.85 wt% silver content.

3.1.5. XPS

The XPS was carried out to investigate the surface compositions and chemical state of Ag_3PO_4 –ATP–Co particles (Fig. 3). The binding energies obtained from the XPS analysis were corrected by referencing C_{1s} to 284.8 eV. The Ag_{3d} spectra of Ag_3PO_4 was composed of two individual peaks at ~ 374 and ~ 368 eV, which could be

Table 1The chemical compositions of ATP, Ag_3PO_4 –ATP–Co, Ag_3PO_4 –ATP–Pr, and recycled Ag_3PO_4 –ATP–Co.

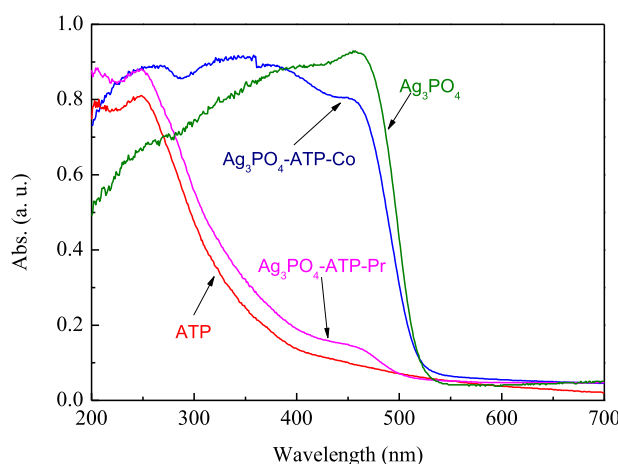
Sample	ATP (%)	Ag_3PO_4 –ATP–Co (%)	Ag_3PO_4 –ATP–Pr (%)	Recycled Ag_3PO_4 –ATP–Co (%)
Si	53.74	42.59	48.52	43.99
Fe	17.85	14.15	16.12	14.61
Mg	12.26	9.72	11.07	10.04
Al	9.7	7.69	8.76	7.94
Ti	1.15	0.91	1.04	0.94
V	0.09	0.07	0.08	0.07
Ba	2.61	2.07	2.36	2.14
Ca	1.13	0.90	1.02	0.93
K	1.04	0.82	0.94	0.85
Na	0.09	0.07	0.08	0.07
Mn	0.1	0.08	0.09	0.08
P	0.16	2.08	1.08	1.56
Ag	0	18.87	8.85	16.78

**Fig. 3.** The XPS spectra of Ag_3PO_4 –ATP–Co particles (Ag 3d).

attributed to $\text{Ag 3d}_{3/2}$ and $\text{Ag 3d}_{5/2}$ binding energies, respectively [19]. The presence of Ag species existed as Ag^+ was confirmed.

3.1.6. UV-vis diffuse reflectance spectrum

UV-vis diffuse reflectance spectra of ATP, Ag_3PO_4 , Ag_3PO_4 –ATP–Co and Ag_3PO_4 –ATP–Pr composites are shown in Fig. 4. Ag_3PO_4 and Ag_3PO_4 –ATP–Co samples both exhibit excellent absorption in the ultraviolet and visible regions with a wavelength shorter than ~ 530 nm as reported by Yi et al. [2]. The Ag_3PO_4 –ATP–Pr composite

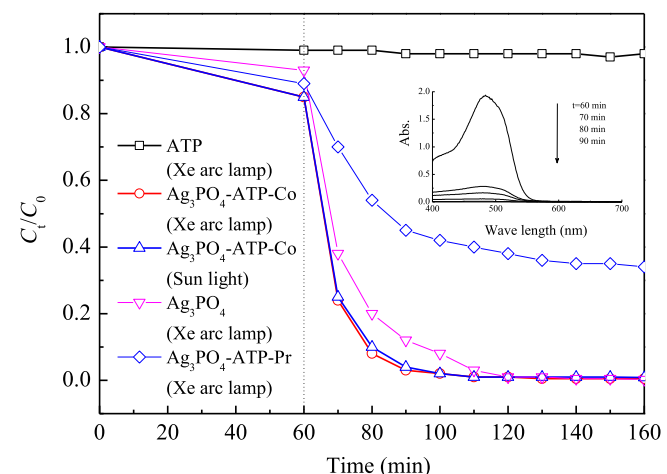
**Fig. 4.** UV-vis adsorption spectra of ATP, Ag_3PO_4 , Ag_3PO_4 –ATP–Co and Ag_3PO_4 –ATP–Pr.

show very weak adsorption in the visible regions, which may cause by its low amount of Ag_3PO_4 on the surface of ATP.

3.2. Photocatalytic performance testing

The photocatalytic properties of ATP, Ag_3PO_4 , Ag_3PO_4 –ATP–Co, and Ag_3PO_4 –ATP–Pr composites were evaluated in terms of the decolorization of Orange II by the photocatalyst under Xe arc lamp or sunlight irradiation. The results are shown in Fig. 5. Almost no reaction occurred in the system with natural ATP exposed to Xe arc lamp for 160 min. The degradation percentages of the solution catalyzed by Ag_3PO_4 –ATP–Co as illuminated by the Xe arc lamp and sunlight were approximately 99% within 90 min, including the adsorption period of 60 min. These results clearly showed that ATP-supported Ag_3PO_4 can be used for degradation under sunlight.

Photocatalytic activation was compared under Xe arc lamp among Ag_3PO_4 , Ag_3PO_4 –ATP–Co, and Ag_3PO_4 –ATP–Pr. The results showed that Ag_3PO_4 –ATP–Co particles were more active than Ag_3PO_4 and Ag_3PO_4 –ATP–Pr particles, which can be attributed to the strong uniformity and smaller Ag_3PO_4 particles dispersed on the ATP. The other reason was the adsorption capacity of ATP. Heterogeneous photocatalytic degradation generally occurs after the reactant is adsorbed on the surface of the catalyst, so adsorption is actually a pre-step for the consequent photocatalytic reaction [20]. ATP is a widely studied adsorbent for organic contaminants removal for its nano-rod-like structure [21,22]. The specific surface areas for Ag_3PO_4 and Ag_3PO_4 –ATP–Co were 23.5 and 365 m^2/g , respectively. This finding indicated that the loading of Ag_3PO_4 on

**Fig. 5.** Photocatalytic degradation of Orange II solution by ATP, Ag_3PO_4 , Ag_3PO_4 –ATP–Co and Ag_3PO_4 –ATP–Pr under Xe light or sunlight.

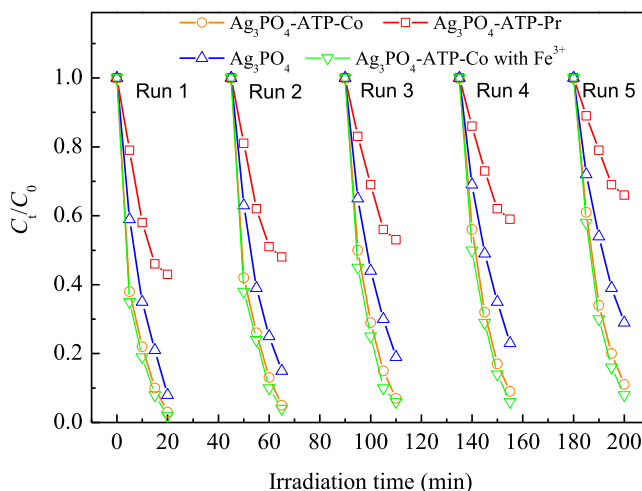


Fig. 6. Repeated photocatalytic degradation of Orange II solution by Ag_3PO_4 , $\text{Ag}_3\text{PO}_4\text{-ATP-Co}$, $\text{Ag}_3\text{PO}_4\text{-ATP-Pr}$ and $\text{Ag}_3\text{PO}_4\text{-ATP-Co}$ with Fe^{3+} (0.1 mol/L) under Xe arc lamp irradiation.

ATP increased the specific surface area for catalysis and the adsorption capacity.

The ATP support improved the catalysis activity and decreased the silver content of the catalysis, which was only 18.87 wt% in $\text{Ag}_3\text{PO}_4\text{-ATP-Co}$ but 77.3 wt% for Ag_3PO_4 ; that is to say that the possible available quantity of Ag in $\text{Ag}_3\text{PO}_4\text{-ATP-Co}$ catalyst was $18.87\% \times 200 \text{ mg} = 37.74 \text{ mg}$, and that in Ag_3PO_4 catalysts was $77.3\% \times 200 \text{ mg} = 154.6 \text{ mg}$. Thus, silver, a noble metal, may be saved by the incorporation of ATP and the cost of treatment may greatly decrease.

3.3. Evaluation of the stability and recyclability of the composites

The stability and recyclability of Ag_3PO_4 under irradiation are important issues related to the use of photocatalysts in water purification (Fig. 6). When Ag_3PO_4 was used as a photocatalyst without a sacrificial reagent, it photo-corroded and decomposed into weakly active Ag during O_2 evolution from water. Its photocatalytic activity then gradually deteriorates, which is the main hindrance for the practical application of Ag_3PO_4 as a recyclable and highly efficient photocatalyst [2]. The recyclability of Ag_3PO_4 , $\text{Ag}_3\text{PO}_4\text{-ATP-Co}$ and $\text{Ag}_3\text{PO}_4\text{-ATP-Pr}$ were compared.

The degradation rates of Orange II as catalyzed by Ag_3PO_4 and $\text{Ag}_3\text{PO}_4\text{-ATP-Co}$ were both high in the first run. However, in the second run, the rate catalyzed by Ag_3PO_4 slightly decreased and became lower than that of $\text{Ag}_3\text{PO}_4\text{-ATP-Co}$. Finally, in the fifth run, the removal efficiency decreased to 71%. The elemental composition of the used $\text{Ag}_3\text{PO}_4\text{-ATP-Co}$ was analyzed, and the results showed that the silver content decreased from 18.87% to 16.78%, indicating that some of the Ag_3PO_4 particles exfoliated from the surface of ATP.

Moreover, $\text{Ag}_3\text{PO}_4\text{-ATP-Pr}$ almost lost its activity after the five runs, which may be explained by silver reduction. The redox potential of the Ag^+/Ag pair was 0.80 V, whereas in the presence of excessive of PO_4^{3-} ions, the redox potential of Ag species markedly decreased to 0.45 V ($\text{Ag}_3\text{PO}_4/\text{Ag}$) [2].

The ATP-loaded Ag_3PO_4 ($\text{Ag}_3\text{PO}_4\text{-ATP-Co}$) showed much higher removal efficiency and stability than free Ag_3PO_4 particles because silver reduction was minimal during light irradiation. This improvement may have resulted from the special structure of ATP. ATP has a special laminated chain structure in which crystalline lattice displacement occurs. Thus, the crystals contain certain quantities of iron, also contains vanadium, barium, titanium and manganese ions in trace amount. Some excited electrons were captured by

these cations on the surface, which inhibited the reduction of silver and increased the stability. The results were verified by adding homogeneous cation (Fe^{3+}) in the degradation of Orange II by $\text{Ag}_3\text{PO}_4\text{-ATP-Co}$. The results show that Fe^{3+} can improve catalytic efficiency. Likewise, the stability of the composites increased, as shown in Fig. 6. The detailed mechanisms should be studied in the future.

4. Conclusion

In this study, a colloidal method for covering silver phosphate on ATP was described. Very fine Ag_3PO_4 crystalline grains ($<5 \text{ nm}$) were obtained on the surface of ATP, which exhibited higher catalytic efficiency than Ag_3PO_4 . The degradation of the solution catalyzed by $\text{Ag}_3\text{PO}_4\text{-ATP-Co}$ under the Xe arc lamp was approximately 99% within 90 min, including an adsorption period of 60 min. The stability also greatly improved with the ATP support. In addition, the silver content in the photocatalyst composite decreased from 77.3 wt% in bare Ag_3PO_4 to 18.8 wt% in the $\text{Ag}_3\text{PO}_4\text{-ATP-Co}$ composite. This facile process for the preparation of $\text{Ag}_3\text{PO}_4\text{-ATP-Co}$ composites can be adopted for the synthesis of other carrier supported Ag_3PO_4 catalysts.

Acknowledgments

This work was supported by the Project of National Natural Science Foundation of China (Grant nos. 21007005 and 21177104), the Project Funded by the Priority Academic Program Development of Jiangsu Higher Education Institutions and Technology Innovation Team of Colleges, and the Universities-Funded Project of Jiangsu Province (no. 2011-24).

References

- [1] C.T. Dinh, T.D. Nguyen, F. Kleitz, T.O. Do, Chemical Communications 47 (2011) 7797–7799.
- [2] Z. Yi, J. Ye, N. Kikugawa, T. Kako, S. Ouyang, H. Stuart-Williams, H. Yang, J. Cao, W. Luo, Z. Li, Y. Liu, R.L. Withers, Nature Materials 9 (2010) 559–564.
- [3] Y. Bi, H. Hu, S. Ouyang, G. Lu, J. Cao, J. Ye, Chemical Communications 48 (2012) 3748–3750.
- [4] X. Cui, Y. Li, Q. Zhang, H. Wang, International Journal of Photoenergy 2012 (2012) 1–6.
- [5] M. Ge, N. Zhu, Y. Zhao, J. Li, L. Liu, Industrial & Engineering Chemistry Research 51 (2012) 5167–5173.
- [6] W. Yao, B. Zhang, C. Huang, C. Ma, X. Song, Q. Xu, Journal of Materials Chemistry 22 (2012) 4050.
- [7] T.A. Vu, C.D. Dao, T.T.T. Hoang, K.T. Nguyen, G.H. Le, P.T. Dang, H.T.K. Tran, T.V. Nguyen, Materials Letters 92 (2013) 57–60.
- [8] J.L. Wang, L.J. Xu, Critical Reviews in Environmental Science and Technology 42 (2011) 251–325.
- [9] Y. Bi, S. Ouyang, J. Cao, J. Ye, Physical Chemistry Chemical Physics 13 (2011) 10071.
- [10] H. Zhang, H. Huang, H. Ming, H. Li, L. Zhang, Y. Liu, Z. Kang, Journal of Materials Chemistry 22 (2012) 10501–10506.
- [11] H. Cui, X. Yang, Q. Gao, H. Liu, Y. Li, H. Tang, R. Zhang, J. Qin, X. Yan, Materials Letters 93 (2013) 28–31.
- [12] L. Zhang, H. Zhang, H. Huang, Y. Liu, Z. Kang, New Journal of Chemistry 36 (2012) 1541–1544.
- [13] J. Ma, J. Zou, L. Li, C. Yao, T. Zhang, D. Li, Applied Catalysis B 134–135 (2013) 1–6.
- [14] J. Cao, G. Shao, Y. Wang, Y. Liu, Z. Yuan, Catalysis Communications 9 (2008) 2555–2559.
- [15] Y. Fang, D. Chen, Materials Research Bulletin 45 (2010) 1728–1731.
- [16] Y. Liu, P. Liu, Z. Su, F. Li, F. Wen, Applied Surface Science 255 (2008) 2020–2025.
- [17] L. Zhang, F. Lv, W. Zhang, R. Li, H. Zhong, Y. Zhao, Y. Zhang, X. Wang, Journal of Hazardous Materials 171 (2009) 294–300.
- [18] A. Khan, M. Qamar, M. Muneer, Chemical Physics Letters 519–520 (2012) 54–58.
- [19] H. Zhang, G. Wang, D. Chen, X. Lv, J. Li, Chemistry of Materials 20 (2008) 6543–6549.
- [20] R.W. Matthews, Journal of Catalysis 113 (1988) 549–555.
- [21] J.H. Huang, X.G. Wang, Q.Z. Jin, Y.F. Liu, Y. Wang, Journal of Environmental Management 84 (2007) 229–236.
- [22] A.L. Xue, S.Y. Zhou, Y.J. Zhao, X.P. Lu, P.F. Han, Journal of Hazardous Materials 194 (2011) 7–14.